Nanoscale

# Dimorphism Shift of Hepatitis B Virus capsids in response to ionic conditions



| | |
|---|---|
| Journal: | *Nanoscale* |
| Manuscript ID | NR-COM-04-2018-003370.R2 |
| Article Type: | Communication |
| Date Submitted by the Author: | 02-Aug-2018 |
| Complete List of Authors: | Sun, Xinyu; The University of Akron, Polymer Science<br>Li, Dong; E O Lawrence Berkeley National Laboratory, Molecular Foundry<br>Wang, Zhaoshuai; University of Kentucky, Pharmaceutical Science<br>Liu, Qiao; The university of akron<br>Wei, Yinan; University of Kentucky, Chemistry<br>Liu, Tianbo; University of Akron, Department of Polymer Science |
| | |

Journal Name

COMMUNICATION

# Dimorphism Shift of Hepatitis B Virus capsids in response to ionic conditions

Received 00th January 20xx,
Accepted 00th January 20xx

DOI: 10.1039/x0xx00000x

www.rsc.org/

Xinyu Sun,[a‡] Dong Li,[a‡] Zhaoshuai Wang,[b] Qiao Liu,[a] Yinan Wei,*[b] Tianbo Liu*[a]

**The dimorphism of HBV capsids (coexistence of *T* = 3 and *T* = 4 capsids) was found to be regulatable by controlling the rate of capsid nucleation using cations such as $K^+$ or $Ca^{2+}$: a quick addition of highly concentrated monovalent and/or multivalent counter-cations resulted in a morphism transition from a thermodynamically more stable, *T* = 4 capsid-dominate state (>80% of total capsids) to a new state containing of ~1:1 amounts of *T* = 3 and *T* = 4 capsids. These results suggested that the salts with strong charge screening ability could narrow the difference in nucleation energy barriers between the two states, which were not inter-convertible once formed. The effect of salts was more significant than other factors such as pH or protein concentration in achieving such a dimorphism shift. The general mechanism of HBV capsid dimorphism described here provides a new perspective in understanding the virus assembly during infection and directing the design of non-infectious capsids for nanotechnology applications.**

Viral capsids are protein shells that protect enclosed viral genome, which play a vital role in virus replication cycle. Most viral capsids are self-assembled from one or several types of capsid proteins via finely balanced, non-covalent protein-protein interactions such as hydrophobic interaction, electrostatic interaction, H-bonding and Van der Waals forces.[1–5] Meanwhile, many viral capsids display polymorphism in their native or non-native states, exhibiting a spontaneous response to peptide truncation, pH, ionic strength or strong core association with nucleic acids or nanoparticles.[6–11] Interestingly, only a few icosahedral viruses, represented by the hepatitis B virus (HBV), have been observed to have the same polymorphism both *in vivo* and *in vitro*, yet the reason for the capsid formation with different structures remains unknown. Understanding the polymorphism of viral capsids will help to elucidate the driving forces for the capsid formation, which has significant impacts towards developing novel anti-viral drugs. The capability of controlling morphology will also provide opportunities for further structural and functional research on the less abundant structures, and provide new strategies for drug-delivery designs and nanostructure fabrications.[12–14]

Hepatitis B virus (HBV) is a liver-tissue-specific enveloped DNA virus and also a causative factor in the development of hepatocellular carcinoma and liver cirrhosis, infecting hundreds of millions of people worldwide.[15] Dimeric HBV core proteins assemble around HBV polymerase and pregenomic RNA into core particles with two sizes: *T* = 3 (R = 16 nm, composed of 180 subunits) and *T* = 4 (R = 18 nm, 240 subunits) icosahedral symmetries.[16] *T* is the triangulation number, which illustrates the number of distinct subunit conformations in organizing an icosahedral structure with 60 *T* subunits.[17] Full-length core protein expressed in *Escherichia coli* can re-assemble into capsids with similar morphology and antigenic properties as the native ones isolated from cell cultures, and still presenting the coexistence of *T* = 3 and *T* = 4 (predominant) structures.[18] The same behavior was observed when the core protein has its C-terminal RNA binding tail truncated to Cp149.[19] Different from many other polymorphic capsids, the dimorphism of HBV capsids endures various assembly conditions. When the assembly of Cp149 dimer was studied *in vitro* in the absence of nucleic acid, only these two morphologies had been observed under a wide range of pH (pH 6.6 to 10.5) and ionic strength (0-1.0 M).[6,20] *T* = 4 structure is the preferred morphology which occupies more than 80% of the total capsids, whereas the *T* = 3 capsid remains as the minority unless a further peptide truncation (to 140-149 residues) is performed, indicating that the C-terminal domain is important in hydrophobic contact so as to stabilize dimers into a preferred state.[6] Other examples of disrupting the distributions of HBV *T* = 3 and *T* = 4 capsids were limited to protein mutation which deprives interdimer disulfide bond, or

[a] Department of Polymer Science, University of Akron, Akron, Ohio, USA. E-mail: tliu@uakron.edu.
[b] Department of Chemistry, University of Kentucky, Lexington, Kentucky, USA. E-mail: Yinan.Wei@uky.edu
†Electronic Supplementary Information (ESI) available. See DOI: 10.1039/x0xx00000x
‡ X. S. and D. L. contributed equally to this work.

below the pseudocritical protein concentration.[21–23] Therefore, it was believed that the wild-type (WT) Cp149 dimers self-assemble into spherical capsids dominated by the *T* = 4 type almost independent of conditions when reaching equilibrium.[6,19]

In this work, we found interestingly that the proportion of *T* = 4 capsids assembled from HBV WT $Cp149_2$ can be lowered from >80% to ~50%, by triggering the capsid nucleation with counterions of different ionic strengths and valences. Investigated under pH 7.5-9.6, self-assemblies from the same amount of $K^+$ ions but different salt addition rates resulted in different *T* = 3 and *T* = 4 capsid populations, revealing the significance of assembly kinetics in determining the final capsid structure.

The theoretical isoelectric point of HBV $Cp149_2$ is 5.05, above which the dimer proteins are negatively charged in solution. For example, each $Cp149_2$ carries ca. -14.5 charges at pH 7.5 (Table S1). HBV capsid proteins are quite soluble in aqueous solution, although they have very hydrophobic patches on the surface (Figure S1). When the dimers self-assemble into capsids, 75% of the buried contact surface is hydrophobic.[24] This short-range attraction is balanced by long-range electrostatic repulsion, which regulates the $Cp149_2$ assembly.[20,25] After introducing additional salts, the cations can screen the strong dimer-dimer repulsion and lower the nucleation energy barrier, driving dimer proteins to assemble into capsids. The increase of the ionic strength facilitates the capsid assembly both kinetically and thermodynamically.[20,24] When $Cp149_2$ assembly was triggered by a relatively low concentration of salt, e.g. 1.0 $mgmL^{-1}$ protein solution titrated quickly with 0.3 M or 0.5 M of buffered KCl (one aliquot addition of salt finishes within 1 s), the overnight reactions exhibited a typical mixture of *T* = 3 and *T* = 4 capsids as the two bands in a 5%-40% buffered sucrose gradient after ultracentrifugation (experimental details in Supporting information). The wider and brighter lower band represented the predominance of *T* = 4 capsids (Figure 1a). Optical density (Figure S2) calculated from the two capsid bands showed that ~80% of total capsids were *T* = 4 capsids at low salt concentrations. pH had a weak effect on the capsid dimorphism, with *T* = 4 capsid fractions varying slightly from 78.8 ± 0.8% to 84.3 ± 3.5% when pH went up from 7.5 to 9.6 (Figure 1b and Table S3). Surprisingly, when 1.0 M of KCl was quickly pipetted into the dimer solution, there was a more remarkable increase in *T* = 3 capsids compared to the *T* = 4 ones, as shown from the higher optical density of the upper protein bands after 24 hours of incubation. The population of *T* = 4 capsids decreased to 53.4 ± 4.7% - 50.9 ± 1.5% in the above pH range (Figure 1a, b, and Table S3). The two capsid bands were collected through side-punctuation for further morphology verification using Transmission Electron Microscope (TEM). Figures 1c and 1d showed that the hollow, spherical particles in the upper and lower bands have an average diameter of D = 26.9 ± 2.3 nm and D = 31.5 ± 2.3 nm, respectively, corresponding to *T* = 3 and *T* = 4 capsids. As an auxiliary evidence, the solutions with mixed assemblies were also examined by the TEM. By randomly counting *T* = 4 particles among capsid mixtures, a drastic drop of *T* = 4 capsids populations to ~50% was also confirmed in 1.0 $mgmL^{-1}$ protein-1.0 M KCl assemblies (striped columns in Figure 1b and Table S3). All assembly reactions were allowed to reach equilibrium for at least 24h before centrifugation and TEM imaging, during which the kinetically trapped pre-capsid intermediates would finish annealing into complete capsids.[22]

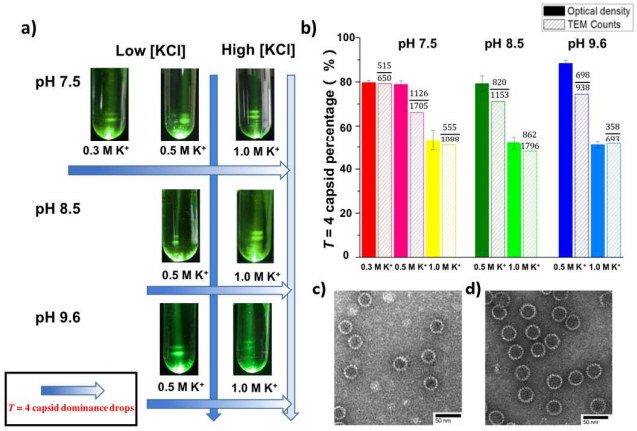


**Figure 1.** Distribution of *T* = 3 and *T* = 4 HBV capsids assembled through quick KCl titration under different pH and salt conditions. a): Assembled mixtures were characterized by a 5-40% sucrose density gradient. Colorless capsid bands were visualized by a 532 nm green laser illuminated from the top. b): The percentage of *T* = 4 capsids was analyzed via the optical density of two capsid bands after sucrose density ultracentrifuge (columns with error bars) and also determined through counting particles from TEM images (striped columns with fractions: denominator represents the counted capsids in total and numerator is the counted *T* = 4 particles). Deviations came from four measurements. c & d): TEM images of *T* = 3 capsids collected from the upper band (c) and *T* = 4 capsids from the lower band (d) after sucrose density centrifugation. Scale bar: 50 nm.

To validate whether this abundance of *T* = 3 capsids is due to a high concentration of salt or a high assembly rate, that is, a thermodynamic or kinetic outcome, a set of control experiments were conducted by incubating protein solutions with the same final salt concentration but with different rates of addition. In contrast to the rapid assembly initiated by introducing a single aliquot of concentrated KCl solution, slow assembly was initiated by a progressive increment of 0.1 M of $K^+$ every 12 h until the same desired final salt concentration was reached. All the solutions were extensively vortexed upon salt addition to avoid inhomogeneous salt concentration. The assembled mixtures incubated with 0.5 M or 1.0 M $K^+$ through these two preparation methods were analyzed and compared by sucrose density gradient, as shown in Figure 2a, and the results were listed in Figure 2b and Table S3. For capsid formation at pH 7.5, both slow and rapid assemblies with 0.5

M $K^+$ favored $T$ = 4 capsids. The stepwise $K^+$ titration gave 83.9 ± 0.9% of $T$ = 4 capsids, while the single-shot titration resulted in a slightly less but still predominant $T$ = 4 particles (78.8 ± 0.8%). As indicated in the previous theoretical calculation, a stronger hydrophobic interaction in the $T$ = 4 capsids contributes to a larger free energy gain upon assembly.[4] Therefore, $T$ = 4 capsids are overwhelmingly formed under a wide range of assembly conditions, especially through slow reactions that drive assemblies to thermodynamic equilibrium. However, we found that the introduction of excessive salt at a high speed largely promote the production of $T$ = 3 capsids. It is interesting that a high concentration of preferred $T$ = 4 capsids was still produced even when [$K^+$] gradually reached 1.0 M, but their yield was only 53.4 ± 4.7% after the single-shot titration of 1.0 M $K^+$ ions. This indicates that although salt ions may affect the contact angle between subunits and result in the change of the shell curvature [26], its contribution is very limited in HBV capsids formation[27] and the capsid dimorphism is not merely a thermodynamic result determined by the final salt concentration. The assembly kinetics was also able to regulate the capsid morphism, and the concentration of counterions in initiating capsid nucleation played the most important role. The assembly of empty HBV capsids begins with the formation of a triangular nucleus. The difference between the $T$ = 3 and $T$ = 4 nuclei conformation is believed to be the true conformational switch. Once assembly begins, this switch becomes locked into a single conformation by the addition of other subunits, leading to the difference in the final $T$ = 3 or $T$ = 4 capsid.[28] A higher salt concentration resulted in faster nucleation by strongly screening the electrostatic repulsion between proteins (Figure S8). Thus, the nucleation energy barrier is lowered, meanwhile the barrier gap between the two nuclei is also narrowed (Figure 2c). In the presence of 1.0 M of $K^+$ ions, the nucleation energy difference between these two nuclei was greatly reduced. Thus $T$ = 3 and $T$ = 4 capsids were assembled in a ratio of about 1:1. The proportion of $T$ = 4 capsids quickly assembled via 0.7 M of $K^+$ was 69.8 ± 1.7%.

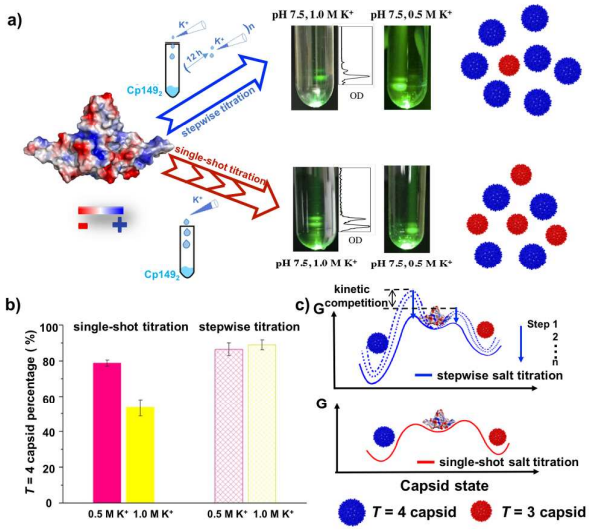


**Figure 2.** Mechanism and sucrose density gradient results of HBV $Cp149_2$ assembly through two ways of salt initiations. a): Stepwise and single-shot titration of 0.5 M KCl (final concentration) into 1.0 $mgmL^{-1}$ protein showed preference for $T$ = 4 capsids. This preference still exits when 1.0 M of $K^+$ was gradually added, but diminished during the rapid assembly initiated by the single-shot addition of 1.0 M $K^+$. Molecular surface of a dimer is colored according to the electrostatic potential (red and blue represent negative and positive, respectively). Deviations came from four measurements. b): The calculated $T$ = 4 capsid fractions through stepwise and single-shot salt additions. c): Energy diagram of HBV capsid formation in response to stepwise titration and single-shot titration of KCl. The activation energy barrier between $T$ = 3 and $T$ = 4 nuclei becomes indistinguishable in the presence of excessive amount of $K^+$, resulting in an almost equal possibility to form $T$ = 3 and $T$ = 4 nuclei.

The different capsid distributions were also verified by the native agarose gel electrophoresis, in which dimers and capsids were separated based on their charges and sizes. As shown in Figure 3, the Cp149 dimers and their assembly mixtures under different reaction conditions were analyzed in lanes 1 to 6. The upper image is a typical Coomassie Blue stained gel image and the lower plots reflect the relative optical density of each protein band on that gel. It can be clearly seen that Cp149 dimers had the highest mobility, while $T$ = 3 capsids moved slower and $T$ = 4 capsids the slowest. Assembled by 1.0 M KCl at pH 7.5, as shown in lane 2 and lane 3, the population of $T$ = 4 particles dropped from 88% to 64% when the addition of $K^+$ ions was accelerated (0.1 M * 10 aliquots at 12 h intervals vs. 0.5 M * 2 aliquots at 30 min. interval). One aliquot addition of 1.0 M $K^+$ ion at pH 8.5 indicated a further decrease to 57%. Again, two titration methods of 0.5 M $K^+$ into protein solutions didn't switch the structure priority, resulting in 90% and 86% of the large particles in the slow and rapid assemblies, respectively. The proportion of $T$ = 3 particles analyzed by the electrophoresis tended to be lower than other in situ characterizations such as sucrose density gradient. Probably, more $T$ = 3 capsids were dissociated into dimers under the electric field due to their lower stability.

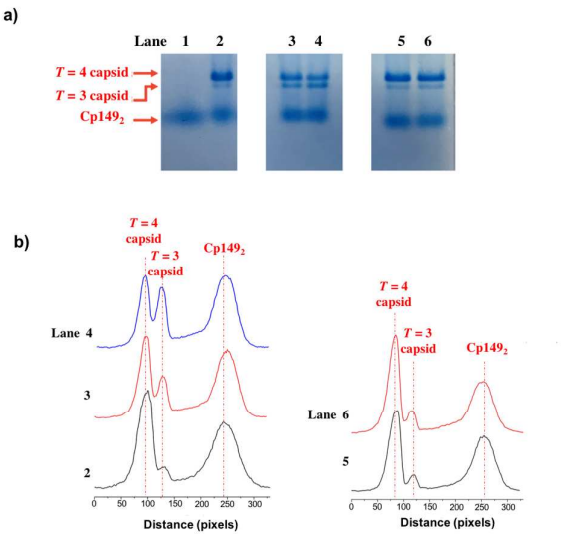


**Figure 3**. Gel electrophoresis results of capsids assembled under different conditions. a): Lane 1: Cp149 dimer; Lane 2: 1.0 mgmL$^{-1}$ protein-1.0 M $K^+$ assembly through stepwise salt addition at pH 7.5; Lanes 3&4:1.0 mgmL$^{-1}$ protein-1.0 M $K^+$ assembly through two aliquots of salt addition at pH 7.5 and single-shot addition at pH 8.5; Lane 5&6: 1.0 mgmL$^{-1}$ protein-0.5 M $K^+$ through stepwise and single-shot salt addition, respectively, at pH 7.5. b): Optical density analysis of the dimer and capsids protein bands in the above agarose gel.

Such an HBV capsid dimorphism distribution change was also observed in response to the single-shot addition of other physiological ions such as $Na^+$ and $Ca^{2+}$. $Na^+$ ion has similar charge screening ability as $K^+$. When increasing the $Na^+$ ion concentration from 0.5 M to 1.0 M to initiate rapid assemblies, the $T$ = 4 capsids also dropped by half in percentage (Figure 4a). $Ca^{2+}$ ions induced the capsid assembly with a four-time lower ionic strength.[29,30] This was believed due to its stronger charge screening ability instead of special binding to the protein.[29] Therefore, we use $Ca^{2+}$ ion as an example to investigate the impact of divalent ions on the capsid dimorphism. Importantly, there was a drastic increase of $T$ = 3 capsids from 6.2 ± 1.1% to 52.1 ± 4.0% merely by varying the $Ca^{2+}$ ion concentration from 10 mM to 30 mM (assembly reaction initiated by quickly pipetting 270 mM buffered $CaCl_2$ stock solution into protein solutions in one aliquot within 1 s; Figures 4a and S4, and Table S3). Therefore, capsids assembled by cations of high valence are particularly sensitive: capsid morphism distribution is changed by a small variation of divalent cations, and the dominance of $T$ = 4 particles can no longer be presumed, which is a new discovery from our study.

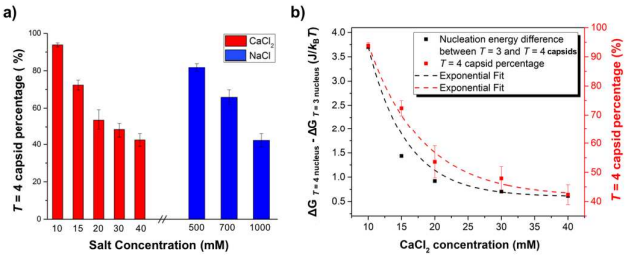


**Figure 4**. a): A decrease in $T$ = 4 capsids percentage with increasing concentration of NaCl or $CaCl_2$ at pH 7.5. Capsids were assembled by a single-shot salt addition. Results were obtained from sucrose density gradient. b): Nucleation energy difference between $T$ = 3 and $T$ = 4 capsids at various $CaCl_2$ concentrations. All these experiments were conducted at an initial protein concentration of 1.0 mgmL$^{-1}$ at pH 7.5.

Comparing the free energy of $T$ = 3 and $T$ = 4 capsid formation and the nucleation energy of their nuclei as a function of salt concentration provides a possible way to understand the dimorphism shift of HBV capsids. Zlotnick and co-workers have shown that the association free energy of capsid formation can be obtained with the knowledge of free dimer and capsid fractions at equilibrium, and the two variables are determined by size exclusion chromatography (SEC).[24] Adapting this method, we further determined the $T$ = 3 and $T$ = 4 capsids fractions using sucrose density gradient. Assuming that all contacts in each $T$ = 3 or $T$ = 4 capsid are identical, the free energy per contact in forming $T$ = 3 and $T$ = 4 capsids can be determined (Details in SI, Figure S3 and Table S2).[31] The contact free energy decreased with increasing ionic strength for both $T$ = 3 and $T$ = 4 capsids, indicating a more favourable process (Table S2). Furthermore, the nucleation energy $\Delta G_*$ can be calculated following the simplified equation derived from the classic nucleation theory[5]

$$\Delta G_* \approx \frac{\left(\frac{\pi c \Delta g}{k_B T}\right)^2}{4 \ln\left(\frac{\rho}{\rho^*}\right)} k_B T \,, \qquad (1)$$

where $c$ denotes the number of empty, non-bounded sites that a rim dimer has compared to a fully-assembled, core dimer protein; $k_BT$ is the product of the Boltzmann constant $k_B$ and the absolute temperature $T$; and $\rho/\rho^*$ is the ratio of total protein number density to the critical assembly protein density; $\Delta g$ represents the binding free energy of a single subunit, which is the product of the association energy per contact and the number of contacts per subunit. The nucleation energy of the $T$ = 3 and $T$ = 4 capsids formation decreases with the addition of salt, and the energy gap between those two shows an exponential decay with the salt concentration (Figure 4b), demonstrating that the selectivity between $T$ = 3 and $T$ = 4 nuclei will be eliminated in the

presence of strong charge screening (very high salt concentration). Since one $T$ = 3 capsid contains 90 dimers and one $T$ = 4 capsid contains 120 dimers, the ratio of the two capsids will be 1.33 to 1, or 42.9% $T$ = 4 capsids in the final mixture. The capsid dimorphism assembled by 40 mM $CaCl_2$ faithfully confirmed this prediction.

In comparison to the charge screening effect through counterions in regulating capsid proteins into different morphology distributions, the effects of protein concentration and/or the assembly pH (protein surface charge) played a much less significant role. Under a wide range of protein concentrations (0.5 - 5.0 $mgmL^{-1}$) in our studies, a close population between $T$ = 3 and $T$ = 4 capsids was always observed through the quick nucleation process (Figure S5 and Table S3). This is probably due to the concentrations we used did not affect the deprotonation of the dimer protein. Also, they were above the threshold which would induce kinetic trap.[28] Even though the assembly environment varied from pH 7.5 to 9.6 (protein surface charge ca. -14.5 to -28.8), single-shot titration of 0.5 M $K^+$ ions always resulted in a $T$ = 4 to $T$ = 3 capsid ratio of 8:2, while the quick assembly via single-shot of 1.0 M $K^+$ ions always produced nearly 1:1 proportion of two capsids (Figure 1 and Table S3).

To further evaluate the effect of protein charge distribution on this kinetically induced dimorphism switch of HBV capsid dimorphism, a mutated $Cp149_2$ protein, D2N/D4N[20], was also investigated. This mutant dimer has the same structural conformation but four fewer charges than the wild-type dimer. Based on the crystalline structure, the mutation sites are not involved in inter-dimer or intra-dimer interactions.[32] The mutant protein can carry the same number of net charge as the WT by adjusting pH, but displaying a different charge distribution. It still exhibited a similar dimorphism distribution change under kinetically controlled assembly (Figure S6), which further confirmed our observation that the nucleation rate affects the capsid morphism. More interestingly, after treating the quickly assembled $T$ = 3 and $T$ = 4 mutant capsids (via 1.0 M KCl) with a disassembly condition by dialyzing away salts at a low temperature and then reassembling them with 0.5 M KCl (Figure S7), a 61.7 ± 1.6% $T$ = 4 capsid solution was switched to a capsid mixture containing 85.0 ± 2.9% $T$ = 4 capsids. Therefore, $Cp149_2$ can assemble reversibly into capsids of $T$ = 3 or $T$ = 4 structures. A previous study on cysteines mutated Cp149 assembly showed that HBV capsid protein without a disulfide bridge assembled into more $T$ = 3 capsids (~40%) than the WT one in the presence of 1.0 M NaCl, probably due to a larger degree of freedom of protein monomers.[21] It is possible that the contribution of the high salt concentration to the observed dimorphic ratio was neglected, as another work on the assembly of Cp149 lacking disulfide bond in 0.3 M NaCl resulted in a regular high $T$ = 4 capsid percentage of 90-95%.[23]

Simulation studies on the virion brome mosaic virus (BMV) have revealed the competition between thermodynamics and kinetics in subunits assembly that led to capsids of different morphologies with the existence of templates,[10] yet the mechanism behind the natural dimorphism of HBV capsids is still under debate.[6,27] Our experimental observations provide clear clues to uncover the kinetic regulation of HBV capsid morphologies between their physiological structures. Especially, the above *in vitro* studies were conducted without protein-nucleic acid interaction or protein conformational change, which revealed the fundamental mechanism of empty capsid assembly. In addition, the lack of monomer exchange between $T$ = 3 and $T$ = 4 capsids at room temperature also suggests that the completely formed capsids will not dissociate to change the polymorphism distribution determined by the nucleation pathway.[33]

## Conclusions

In summary, a preference change of HBV capsid dimorphism in their native states was discovered through the regulation of counterion-mediated nucleation. The energy barrier between the $T$ = 4 and $T$ = 3 nuclei was changed in response to the solution ionic strength and the type of cations, which shifted the capsid size distribution. The effects of salt concentration, the rate of salt introduction, and the cation valence were much more significant than other factors such as pH (protein surface charge) and protein concentration in this dimorphism regulation. Our research provided an in-depth fundamental understanding of polymorphism in viral capsid formation, which will be of potential interests in developing novel anti-viral drugs through the assembly interference, as well as inspiring non-infectious capsid based nanotechnologies. The kinetics regulation and counterion-mediated nucleation can be further applied to inspire and understand other protein complexes and polyelectrolyte assembly systems.

## Conflicts of interest

There are no conflicts to declare.

## Acknowledgements

T.L. acknowledges support from the National Science Foundation (CHE-1607138) and The University of Akron. We also acknowledge Krutika Invally from Dr. Lu-Kwang Ju's group in the Department of Chemical and Biomolecular Engineering, The University of Akron, for her help with the SEC measurement.

## Notes and references

1 A. Šiber and R. Podgornik, *Phys. Rev. E*, 2008, **78**, 51915.
2 J. Kim and J. Wu, *J. Chem. Phys.*, 2014, **140**, 06B612_1.
3 S. C. Harrison, *Fields' Virol.*, 2007, **1**, 59.
4 R. F. Bruinsma, W. M. Gelbart, D. Reguera, J. Rudnick and R. Zandi, *Phys. Rev. Lett.*, 2003, **90**, 248101.
5 R. Zandi, P. van der Schoot, D. Reguera, W. Kegel and H. Reiss, *Biophys. J.*, 2006, **90**, 1939–1948.

6 A. Zlotnick, N. Cheng, J. F. Conway, F. P. Booy, A. C. Steven, S. J. Stahl and P. T. Wingfield, *Biochemistry*, 1996, **35**, 7412–7421.
7 D. M. Salunke, D. L. Caspar and R. L. Garcea, *Biophys. J.*, 1989, **56**, 887–900.
8 L. Lavelle, M. Gingery, M. Phillips, W. M. Gelbart, C. M. Knobler, R. D. Cadena-Nava, J. R. Vega-Acosta, L. A. Pinedo-Torres and J. Ruiz-Garcia, *J. Phys. Chem. B*, 2009, **113**, 3813–3819.
9 M. A. Krol, N. H. Olson, J. Tate, J. E. Johnson, T. S. Baker and P. Ahlquist, *Proc. Natl. Acad. Sci.*, 1999, **96**, 13650–13655.
10 O. M. Elrad and M. F. Hagan, *Nano Lett.*, 2008, **8**, 3850–3857.
11 J. Tang, J. M. Johnson, K. A. Dryden, M. J. Young, A. Zlotnick and J. E. Johnson, *J. Struct. Biol.*, 2006, **154**, 59–67.
12 S. J. Stray and A. Zlotnick, *J. Mol. Recognit.*, 2006, **19**, 542–548.
13 S. P. Katen, Z. Tan, S. R. Chirapu, M. G. Finn and A. Zlotnick, *Structure*, 2013, **21**, 1406–1416.
14 C. J. Schlicksup, J. C.-Y. Wang, S. Francis, B. Venkatakrishnan, W. W. Turner, M. VanNieuwenhze and A. Zlotnick, *Elife*, 2018, **7**, e31473.
15 T. J. Liang, *Hepatology*.
16 F. Birnbaum and M. Nassal, *J. Virol.*, 1990, **64**, 3319–3330.
17 D. L. D. Caspar and A. Klug, in *Cold Spring Harbor symposia on quantitative biology*, Cold Spring Harbor Laboratory Press, 1962, vol. 27, pp. 1–24.
18 R. A. Crowther, N. A. Kiselev, B. Böttcher, J. A. Berriman, G. P. Borisova, V. Ose and P. Pumpens, *Cell*, 1994, **77**, 943–950.
19 P. T. Wingfield, S. J. Stahl, R. W. Williams and a C. Steven, *Biochemistry*, 1995, **34**, 4919–4932.
20 X. Sun, D. Li, Z. Wang, P. Yin, R. Hu, H. Li, Q. Liu, Y. Gao, B. Ren and J. Zheng, *ACS Omega*, 2018, **3**, 4384–4391.
21 A. Zlotnick, I. Palmer, J. D. Kaufman, S. J. Stahl, A. C. Steven and P. T. Wingfield, *Acta Crystallogr. Sect. D Biol. Crystallogr.*, 1999, **55**, 717–720.
22 Z. D. Harms, L. Selzer, A. Zlotnick and S. C. Jacobson, *ACS Nano*, 2015, **9**, 9087–9096.
23 L. Selzer, S. P. Katen and A. Zlotnick, *Biochemistry*, 2014, **53**, 5496–5504.
24 P. Ceres and A. Zlotnick, *Biochemistry*, 2002, **41**, 11525–11531.
25 W. K. Kegel and P. van der Schoot, *Biophys. J.*, 2004, **86**, 3905–3913.
26 J. Wagner and R. Zandi, *Biophys. J.*, 2015, **109**, 956–965.
27 P. Moerman, P. Van Der Schoot and W. Kegel, *J. Phys. Chem. B*, 2016, **120**, 6003–6009.
28 A. Zlotnick, J. M. Johnson, P. W. Wingfield, S. J. Stahl and D. Endres, *Biochemistry*, 1999, **38**, 14644–14652.
29 S. J. Stray, P. Ceres and A. Zlotnick, *Biochemistry*, 2004, **43**, 9989–9998.
30 Y. Choi, S. G. Park, J. Yoo and G. Jung, *Virology*, 2005, **332**, 454–463.
31 S. Katen and A. Zlotnick, *Methods Enzymol.*, 2009, **455**, 395–417.
32 S. A. Wynne, R. A. Crowther and A. G. W. Leslie, *Mol. Cell*, 1999, **3**, 771–780.
33 A. J. R. Heck, 2010, **12**, 13368–13371.

## TOC:

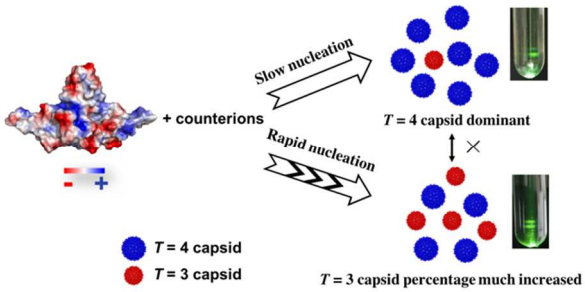


HBV capsid dimorphism regulation through manipulating the rate of capsid nucleation using highly concentrated and/or multivalent counter-cations.